Int. J. Heat Mass Transfer. Vol. 25, No. 3, pp. 363–370, 1982
Printed in Great Britain

0017–9310/82/030363 08 $03.00/0
Pergamon Press Ltd.

THERMAL CONVECTION IN A HORIZONTAL FLUID LAYER HEATED INTERNALLY AND FROM BELOW

YOSHIHIRO KIKUCHI, TERUFUMI KAWASAKI and TSUTOMU SHIOYAMA
Department of Nuclear Engineering, Kyoto University, Sakyo-ku, Kyoto, Japan

(*Received* 23 *May* 1981)

Abstract—This paper deals with the experimental results of turbulent thermal convection in a horizontal water layer with uniform volumetric energy sources and a constant rate of bottom heating. The experimental data were compared with a simple boundary layer analysis which expressed the upper and the lower surface modified Nusselt numbers as functions of two independent Rayleigh numbers, based respectively on the volumetric heating rate and the surface-to-surface temperature difference. A practical correlation equation was derived for the bulk core temperature depending upon a single dimensionless parameter which measures the relative rates of internal and external heating.

NOMENCLATURE

a, thermal diffusivity;
c, proportionality constant in equations (3) and (6);
g, gravitational acceleration;
G, proportionality constant in equations (22) and (25);
H, constant exponent in equations (22) and (25);
L, layer depth;
m, constant exponent in equations (3) and (6);
Nu_E, external Nusselt number, $qL/\lambda\Delta T$;
Nu_I, internal Nusselt number, $QL^2/\lambda\Delta T$;
$Nu\dagger$, modified Nusselt number, $2q/QL$;
q, heat flux;
Q, volumetric rate of energy generation;
r^2, coefficient of correlation;
Ra_E, external Rayleigh number, $g\beta\Delta TL^3/av$;
Ra_I, internal Rayleigh number, $g\beta QL^5/2\lambda av$;
T, temperature;
ΔT, surface-to-surface temperature difference, $T_0 - T_1$;
X, dimensionless distance, z/L;
z, vertical coordinate, $0 \leqq z \leqq L$.

Greek symbols

α, proportionality constant in equation (18);
β, isobaric coefficient of volumetric expansion;
γ, constant exponent in equation (18);
δ, thermal boundary layer thickness;
θ, dimensionless temperature, $(T - T_1)/\Delta T$;
λ, thermal conductivity;
v, kinematic viscosity;
ϕ, dimensionless parameter defined in equation (35).

Subscripts

E, external;
I, internal;
δ, boundary layer;
0, lower surface;
1, upper surface.

INTRODUCTION

THERMAL convection in a fluid with distributed energy sources appears widely in geophysics, astrophysics and engineering. Thermal convection driven by energy sources has been proposed as a mechanism for the earth's mantle [1–3] and for the outer region of stellar interiors [4]. Engineering processes where there is heat generation by a chemical or nuclear reaction within the fluid are common today, and correct process design often requires accurate correlations for heat transfer coefficient at boundary surfaces. On this last point, it is indispensable from reactor safety considerations to be able to predict the probable magnitude of thermal convective heat transfer with volumetric heat release in relation to post-accident heat removal (PAHR) in a liquid metal fast breeder reactor (LMFBR).

Despite its relevance to many important technological and physical problems, thermal convection with volumetric energy sources has scarcely been studied both analytically and experimentally. Most past studies have been conducted under an adiabatic [5, 6] or cooling [7] conditions at the lower boundary of a horizontal fluid layer. So far, there exist very few works, except the theoretical study of Cheung [8], which treat the combined effects of heating internally and from below on thermal convection in a horizontal fluid layer. This led the present authors to carry out an experimental study of turbulent thermal convection in a horizontal fluid layer heated internally and from below (combined internal and external heating).

The experimental results will be compared with a simple boundary layer analysis which expresses the upper and the lower surface modified Nusselt numbers as functions of two independent Rayleigh numbers, based respectively on the surface-to-surface temperature difference and the volumetric heating rate. In addition, a simple correlation will be given for predicting the bulk core temperature in many practical applications.

EXPERIMENTAL APPARATUS AND PROCEDURE

A schematic diagram of the experimental apparatus is shown in Fig. 1. The convection chamber consisted of a fluid layer of a dilute aqueous potassium chloride solution bounded by two copper plates, which served as electrodes for the passage of electric current through the layer. The overall dimensions of the fluid layer were 200 × 200 mm, and layer depths were varied from 29 to 98 mm. Four side walls were made of 10 mm thick acrylic resin. A 60 mm thick insulator was equipped to keep the side walls in an adiabatic condition.

The temperature of the upper boundary of the layer was held constant with thermostatically controlled water circulating through a cooling tank, which was soldered to the back of the copper plate (6 mm in thickness). Water was pumped to the cooling tank from a bath. In order to heat the layer from below, a Nichrome-resistance bottom heater was fastened to the underside of a 1.6 mm thick aluminum plate, which was bolted to the back of the copper plate (10 mm in thickness). The aluminum plate was electrically insulated from the copper plate by a 2 mm thick Bakelite plate to evaluate the heat flux to the layer from below.

Twelve Chromel–Alumel thermocouples were used to monitor the temperatures of copper plates. The thermocouple grooves in the plates were drilled to within 2 mm of the surface in contact with the test fluid. After the thermocouples were set, the grooves were filled with solder. For temperature measurements of the fluid layer, a small vinyl-coated thermocouple (0.5 mm in diameter) was used, which could be traversed vertically with a movement device.

Alternating electrical current was supplied from two line voltage regulators to the fluid and the bottom heater independently. Each dissipated power was measured with a voltmeter–ammeter combination system with a 1% rated accuracy.

Prior to each experiment, all inner surfaces of the convection chamber were thoroughly cleaned. After the working fluid was poured into the chamber, the horizontal alignment of the chamber was adjusted with a spirit level. The experiments were then performed in the following manner. Power was supplied to the fluid layer and the bottom heater. In order to maintain the upper surface at a constant temperature, water was circulated into the cooling tank. The fluid layer was held nearly at room temperature during the experiment in order to minimize heat losses. The output signals from thermocouples, which measured the temperatures of the lower and upper plates, both sides of the Bakelite plate and the fluid layer, were recorded on a strip chart. Sufficient time was allowed for the convection development to reach a steady state condition. Upon reaching a steady state all the temperature readings were taken and averaged by a multichannel digital voltmeter, which was controlled by a microcomputer. Another two sets of temperature readings were taken 10 and 20 minutes later, and when good agreement was reached within 0.1 K for each set of temperature readings, data were recorded.

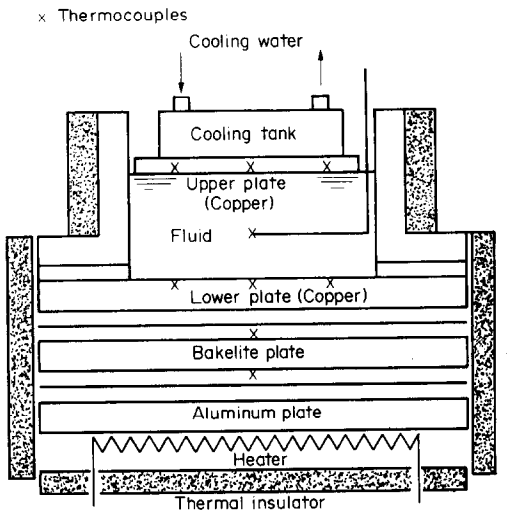

FIG. 1. Experimental apparatus.

RESULTS AND DISCUSSIONS

1. *External heating case*

In order to establish a base case, experiments were first carried out with a bottom-heated fluid layer without internal energy sources. In this conventional external heating case, the external Nusselt number is defined in terms of the layer depth, L, as

$$Nu_E \equiv \frac{q}{\lambda \Delta T/L} \tag{1}$$

where q is the heat flux to the fluid. The external Rayleigh number is defined in terms of this same length and the surface-to-surface temperature difference, as

$$Ra_E \equiv \frac{g\beta \Delta T L^3}{a\nu}. \tag{2}$$

Figure 2 shows the relation between the external Nusselt number and the external Rayleigh number. Although data are slightly scattered, the external Nusselt numbers correlate well with the external Rayleigh numbers assuming a relation of the form

$$Nu_E = c_E Ra_E^{m_E} \tag{3}$$

The resulting heat transfer correlation is

$$Nu_E = 0.130\, Ra_E^{0.290},$$
$$2.2 \times 10^6 \leqq Ra_E \leqq 1.1 \times 10^8. \tag{4}$$

The correlation is obtained by a linear regression of $\ln(Nu_E)$ vs $\ln(Ra_E)$ through 9 points. The coefficient of correlation r^2 is 0.970. In Fig. 2 are also indicated the correlations obtained by Chu and Goldstein [9] and Garon and Goldstein [10]. The present experimental results agree fairly well with those two correlations.

2. *Internal heating case*

In the second series of experiments, however, the fluid layer was internally heated under an adiabatic lower surface condition. In this internal heating case,

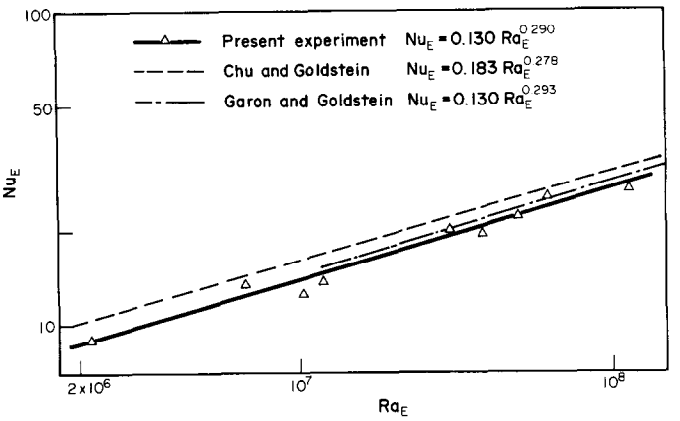

FIG. 2. Thermal convective heat transfer data and correlation equations in external heating case.

the internal Rayleigh number and the internal Nusselt number at the upper surface are defined as

$$Ra_I \equiv \frac{g\beta QL^5}{2\lambda a v} \quad \text{and} \quad Nu_I \equiv \frac{QL^2}{\lambda \Delta T} \tag{5}$$

respectively where Q is the rate of volumetric heat generation in the fluid. Figure 3 shows that the experimental results of the internal Nusselt number correlate well with the internal Rayleigh number assuming a relation of the form

$$Nu_I = c_I Ra_I^{m_I}. \tag{6}$$

The linear regression of ln (Nu_I) on ln (Ra_I) gives

$$Nu_I = 0.365\ Ra_I^{0.238},$$
$$2.3 \times 10^6 \leqq Ra_I \leqq 3.5 \times 10^9,$$
$$r^2 = 0.998, \quad 12 \text{ observations.} \tag{7}$$

In Fig. 3 the experimental results of Kulacki and Nagle [5] and Fiedler and Wille [6] are compared with the present data. The present results are in good agreement with these data.

Figure 4 shows the relationship between the internal (Ra_I) and external (Ra_E) Rayleigh numbers in the internal heating case. Ra_I appears to be strongly dependent upon Ra_E. A linear regression of ln (Ra_I) on ln (Ra_E) gives

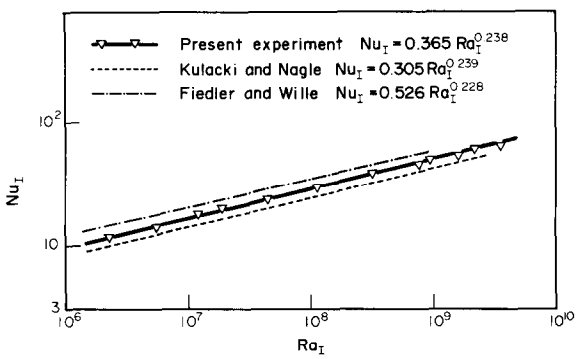

FIG. 3. Thermal convective heat transfer data and correlation equations in internal heating case.

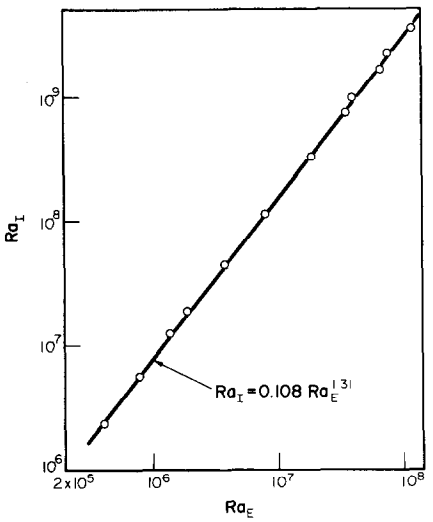

FIG. 4. Relation between internal Rayleigh number and external Rayleigh number in internal heating case.

$$Ra_I = 0.108\ Ra_E^{1.31},$$
$$4.1 \times 10^5 \leqq Ra_E \leqq 1.1 \times 10^8,$$
$$2.3 \times 10^6 \leqq Ra_I \leqq 3.5 \times 10^9,$$
$$r^2 = 0.9997, 12 \text{ observations.} \tag{8}$$

Equation (8) can also be obtained from equation (7) combined with the following variation of Nu_I:

$$Nu_I = \frac{QL^2}{\lambda \Delta T} = 2\frac{QL^2}{2\lambda \Delta T} = 2\frac{Ra_I}{Ra_E}. \tag{9}$$

3. Combined internal and external heating case

The third series of experiments was carried out with a fluid layer heated simultaneously from within and from below. Figure 5 shows typical measured temperature profiles in the layer for $0 \leqq Ra_I \leqq 2.17 \times 10^9$ at nearly constant Ra_E. The horizontal axis θ is the dimensionless temperature difference, $(T - T_1)/(T_0 - T_1)$ where T_0 and T_1 are the lower and the upper surface temperatures, respectively. The vertical

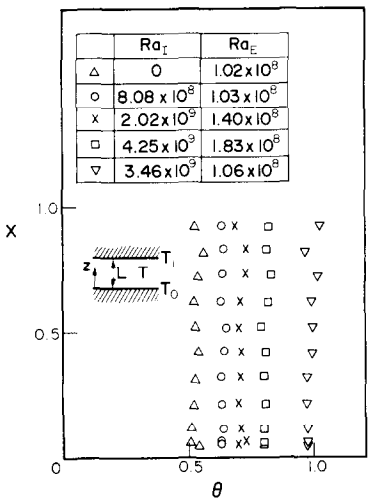

FIG. 5. Dimensionless temperature distributions in horizontal fluid layer.

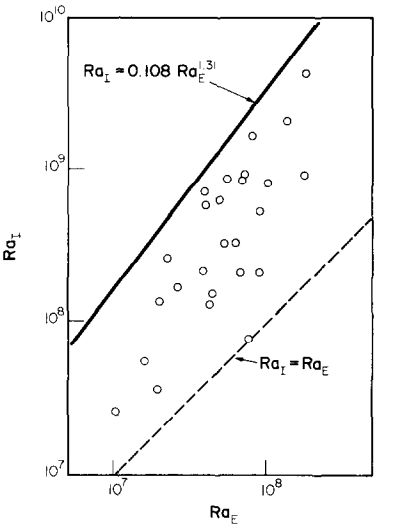

FIG. 6. Range of experimental conditions in combined heating case: Ra_I–Ra_E space.

axis X is the dimensionless distance, z/L where L is the layer thickness.

It can be seen from the figure* that for every Ra_I and Ra_E the central core region is nearly isothermal because of strong turbulent mixing, and that the fluid temperature varies markedly only in thin boundary layers near each surface. In this figure other different cases are also indicated; (a) external heating and (b) internal heating. For the external heating case in which there are no volumetric energy sources, i.e. $Ra_I = 0$, the dimensionless bulk core temperature θ_b is nearly one-half. This means that the isothermal core region is at a temperature of approximately the arithmetic mean between T_0 and T_1. When internal heating is added to the layer, i.e. $Ra_I \neq 0$, the situation is quite different. In this case, the fluid layer is heated internally and from below (combined internal and external heating). As Ra_I increases, θ_b increases from one-half and an asymmetry in the temperature field becomes more pronounced. At sufficiently high Ra_I, θ_b reaches unity and an adiabatic condition is then established at the lower surface. There is virtually no thermal boundary layer at the bottom of the layer.

The above-mentioned fact therefore leads us to say that the external heating case is an extreme situation where Ra_I approaches zero in the combined heating case, and that the case in which there is an internal heating of the layer with an adiabatic lower surface is the other extreme situation, in which Ra_I depends upon the corresponding value of Ra_E through the correlation given by equation (8).

In the combined heating case, there are two independent variables, external Rayleigh number Ra_E and internal Rayleigh number Ra_I. Figure 6 carries plots of the present data in the Ra_I–Ra_E space. All the points exist in the region of $Ra_E \leqq Ra_I \leqq 0.108 Ra_E^{1.31}$. The range of external and internal Rayleigh numbers is $1.1 \times 10^7 \leqq Ra_E \leqq 1.8 \times 10^8$; $2.6 \times 10^7 \leqq Ra_I \leqq 4.3 \times 10^9$. Under these experimental conditions the internal heat generation effect is more dominant than the external heating.

To the present authors' knowledge there is only the experimental work of Suo-Anttila and Catton [11] on the turbulent thermal convection problem in a horizontal fluid layer with combined internal and external heating. But only a few data points were obtained in their experiments since the purpose of their work was to investigate the effect of unequal surface temperatures on a volumetrically heated fluid layer cooled from below and consequently most of their measurements were performed under bottom cooling conditions.

On the other hand, Cheung [8] studied analytically the combined heating fluid layer by a simple boundary layer approach. He first assumed that, for the external heating case, the relationship between a boundary layer Rayleigh number Ra_δ and a dimensionless boundary thickness δ/L is represented by a correlation of the form

$$Ra_\delta = 53.1\,(\delta/L)^{-0.391} \tag{10}$$

where, with $\Delta T_\delta = \Delta T/2$, Ra_δ and δ are defined as

$$Ra_\delta \equiv \frac{g\beta\Delta T_\delta \delta^3}{av} \quad \text{and} \quad \delta \equiv \frac{\lambda \Delta T_\delta}{q}. \tag{11}$$

Similarily, for the internal heating case, the Ra_δ and δ/L relationship is represented by

$$Ra_\delta = 106.2\,(\delta/L)^{-0.391}. \tag{12}$$

In this situation $\Delta T_\delta = \Delta T$ should be assumed instead of $\Delta T_\delta = \Delta T/2$.

* In Fig. 5 data are eliminated in the boundary layer to avoid the plots from lying one upon another and to clarify the development of turbulent convection.

Figure 7 shows a comparison of both equations (10) and (12) with the present experimental results which are derived from equations (4) and (7). A discrepancy is seen to occur in both cases; (a) external heating and (b) internal heating. This may be attributed to the fact that it is difficult to determine correctly the Ra_δ and δ/L relationship by the experimental results presented in the conventional Nu–Ra correlation since the plot of Ra_δ vs δ/L tends to amplify the differences among various measured data. A new analysis is, therefore, needed to derive a heat transfer correlation expression for the combined internal and external heating case.

Following the conventional definition of Nusselt number, i.e. Nu $\sim q_{\text{actual}}/q_{\text{conductive}}$, the surface heat transfer can be written as

$$Nu_1 = \frac{q_1}{\lambda\Delta T/L + QL/2}$$

$$\text{and} \quad Nu_0 = \frac{q_0}{\lambda\Delta T/L - QL/2} \tag{13}$$

where subscripts 1 and 0 denote the upper and the lower surfaces, respectively. It is noted that Nu_0 has a discontinuity point at $\lambda\Delta T/L = QL/2$, i.e. $Ra_1 = Ra_E$. In the subsequent analysis, therefore, the present data are rearranged with the modified Nusselt numbers

$$Nu_1\dagger \equiv \frac{q_1}{QL/2} \quad \text{and} \quad Nu_0\dagger \equiv \frac{q_0}{QL/2}, \quad Q > 0. \tag{14}$$

The relation between $Nu_0\dagger$ and $Nu_1\dagger$ is obtained from conservation of energy, i.e. $q_1 = q_0 + QL$, as the following equation

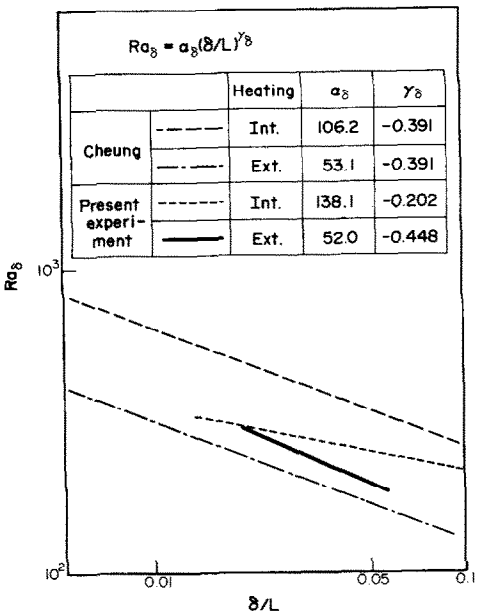

FIG. 7. Experimental data and correlation equations derived from Cheung's boundary layer theory.

$$Nu_1\dagger - Nu_0\dagger = 2. \tag{15}$$

From the measured temperature distributions indicated earlier in Fig. 5, thin thermal boundary layers are seen to be fully developed near the upper and the lower surfaces. This boundary layer-dominant aspect is employed in the present study, which is similar to Cheung's concept. From dimensional considerations, a boundary layer thickness δ and a boundary layer Rayleigh number Ra_δ can be defined as the following equations

$$\delta \equiv \lambda\Delta T_\delta/q, \tag{16}$$

$$Ra_\delta \equiv \frac{g\beta\Delta T_\delta \delta^3}{av} = Ra_E\left(\frac{\Delta T_\delta}{\Delta T}\right)\left(\frac{\delta}{L}\right)^3 \tag{17}$$

where ΔT_δ is the temperature difference across the boundary layer and ΔT the surface-to-surface temperature difference, $T_0 - T_1$, which is applied to the definition of external Rayleigh number Ra_E. In the above equations, the effects of heat generation within the thin thermal boundary layers have been neglected.

The relationship between δ and Ra_δ is assumed as

$$Ra_\delta = \alpha_\delta(\delta/L)^{\gamma_\delta} \tag{18}$$

where α_δ and γ_δ are intended to be constant. Since δ/L corresponds to the conventional Nusselt number [equation (16)] and Ra_δ is proportional to Ra_E [equation (17)], equation (18) corresponds to the relationship for the external heating case, $Nu_E = c_E Ra_E^{m_E}$. Namely, it is intended that for the combined heating case the heat transfer behavior in the boundary layer is treated with a similar conventional correlation. In turbulent convection the sum of temperature differences across the individual boundary layers, $\Delta T_{\delta_0} + \Delta T_{\delta_1}$, must be equal to ΔT. In terms of the dimensionless bulk core temperature θ_b, we obtain

$$\Delta T_{\delta_1} = \theta_b\Delta T \quad \text{and} \quad \Delta T_{\delta_0} = (1 - \theta_b)\Delta T \tag{19}$$

From equations (16) and (17), the lower boundary layer thickness δ_0 can be related to θ_b and Ra_E by

$$(\delta_0/L)^{-1} = \left(\frac{Ra_E(1 - \theta_b)}{\alpha_{\delta_0}}\right)^{1/(3-\gamma_{\delta_0})} \tag{20}$$

Substituting equations (16) and (19) into equation (14), we obtain

$$Nu_0\dagger = \frac{Ra_E}{Ra_1}\frac{(1 - \theta_b)}{\delta_0/L}, \quad Ra_1 > 0. \tag{21}$$

Combination of equations (20) and (21) yields, after rearrangement, the heat transfer correlation at the lower surface

$$Nu_0\dagger\, Ra_1 = G_0\,[Ra_E(1 - \theta_b)]^{H_0} \tag{22}$$

where

$$G_0 = \left(\frac{1}{\alpha_{\delta_0}}\right)^{1/(3-\gamma_{\delta_0})} \quad \text{and} \quad H_0 = 1 + \frac{1}{3 - \gamma_{\delta_0}}. \tag{23}$$

Similarily for the upper boundary layer, we obtain, after some manipulations,

$$Nu_1\dagger = \frac{Ra_E}{Ra_l}\frac{\theta_b}{\delta_1/L}, \quad Ra_l > 0, \tag{24}$$

$$Nu_1\dagger\, Ra_l = G_1\,[Ra_E\theta_b]^{H_1} \tag{25}$$

and

$$G_1 = \left(\frac{1}{\alpha_{\delta_1}}\right)^{1/(3-\gamma_{\delta_1})} \quad \text{and} \quad H_1 = 1 + \frac{1}{3-\gamma_{\delta_1}}. \tag{26}$$

The constants G_0, H_0, G_1 and H_1 will be directly determined with the use of experimental data in the $Nu\dagger - Ra$ space since the plot of Ra_δ vs δ/L tends to amplify the small differences among various measured data. Figure 8 shows the relationship between $Nu_0\dagger Ra_l$ and $Ra_E(1-\theta_b)$ in the present measurements. A linear regression of ln $[Nu_0\dagger\, Ra_l]$ vs ln $[Ra_E(1-\theta_b)]$ through 25 data points is

$$Nu_0\dagger\, Ra_l = 0.257\,[Ra_E(1-\theta_b)]^{1.31}, \quad r^2 = 0.984. \tag{27}$$

Similar relationship between $Nu_1\dagger\, Ra_l$ and $Ra_E\theta_b$ is shown in Fig. 9. A linear regression of ln $[Nu_1\dagger\, Ra_l]$ vs ln $[Ra_E\theta_b]$ is

$$Nu_1\dagger\, Ra_l = 0.201\,[Ra_E\theta_b]^{1.31}, \quad r^2 = 0.993. \tag{28}$$

Consequently, G_0, H_0, G_1 and H_1 have been determined well as constants. This suggests that the assumption given by equation (18) is valid in both the upper and the lower boundary layers for the combined heating case.

From equations (15), (27) and (28) the dimensionless bulk core temperature θ_b can be related to two independent parameters Ra_E and Ra_l by

$$0.201\,[Ra_E\theta_b]^{1.31} - 0.257\,[Ra_E(1-\theta_b)]^{1.31} = 2Ra_l. \tag{29}$$

Graphical representations of these correlations are shown in Figs. 10 and 11. In Fig. 10, θ_b is given as a function of Ra_l and Ra_E. In Fig. 11, on the other hand, the dependency of $Nu_1\dagger$ upon Ra_l and Ra_E is given, and then $Nu_0\dagger$ can be easily obtained through equation (15).

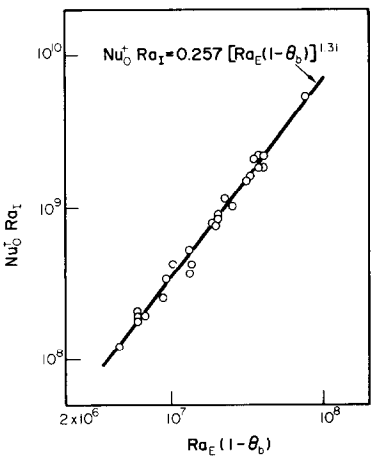

FIG. 8. Generalized heat transfer correlation at lower surface in combined heating case.

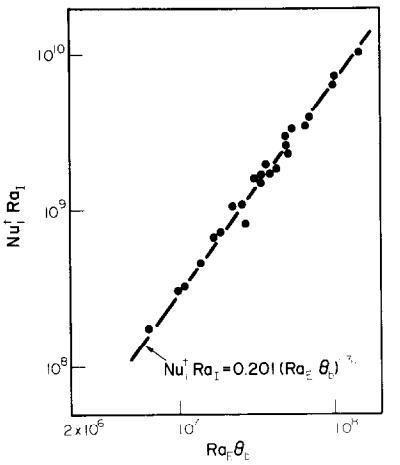

FIG. 9. Generalized heat transfer correlation at upper surface in combined heating case.

As pointed out earlier, the external and the internal heating cases can be considered as the extreme situations in the combined heating case. Equations (22) and (25) will be applied to these extreme cases to verify a consistency of heat transfer correlations obtained in the combined heating case. In the external heating case θ_b is one-half, and then both δ_0/L and δ_1/L are equal to $1/2Nu_E$. Application of these relations to equations (21) and (24) approaches a limit for the heat transfer correlations at the lower and the upper surfaces:

$$Nu_0\dagger\, Ra_l\left(=\frac{Ra_E(1-\theta_b)}{\delta_0/L}\right)\to Nu_E\, Ra_E$$

and (30)

$$Nu_1\dagger\, Ra_l\left(=\frac{Ra_E\,\theta_b}{\delta_1/L}\right)\to Nu_E\, Ra_E.$$

According to the correlation given by the experimental data, G_0, H_0, G_1 and H_1 are determined as constants for the combined heating case. If the assumption that G_0, H_0, G_1 and H_1 are constant all over the domain from the external heating to the internal heating, these values can be predicted from the heat transfer correlation in the extreme situation, i.e. $Nu_E = c_E Ra_E^{n_1}$. Substituting equation (4) into equations (22) and (30), we obtain $G_0 = 0.318$ and $H_0 = 1.29$, which differ a little from the values ($G_0 = 0.257$ and $H_0 = 1.31$) given in equation (27).

In the internal heating case, on the other hand, the upper surface heat flux q_1 is equal to QL and the dimensionless bulk core temperature θ_b is unity. Consequently, equation (25) reached the following expression

$$2Ra_l = G_1 Ra_E^{H_1}. \tag{31}$$

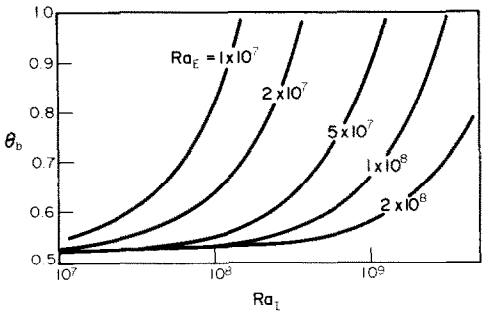

FIG. 10. Effect of internal and external Rayleigh numbers on dimensionless turbulent core temperature.

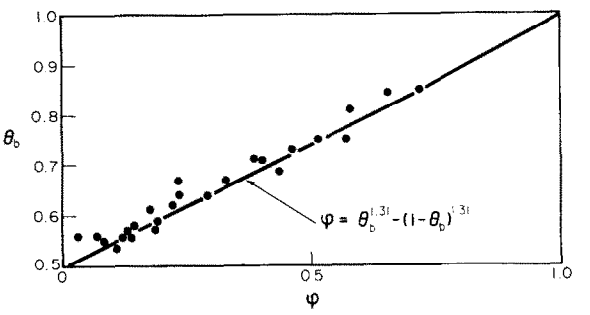

FIG. 12. Variation of dimensionless turbulent core temperature under different heating conditions.

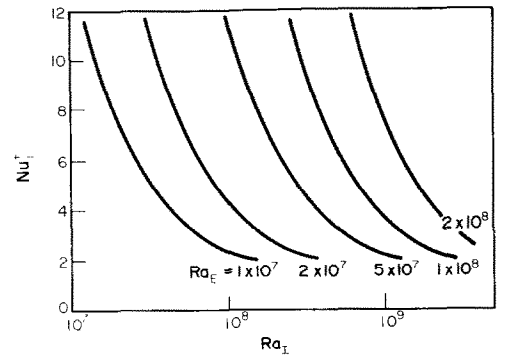

FIG. 11. Effect of internal and external Rayleigh numbers on modified Nusselt number at upper surface.

From equations (8) and (31), we obtain $G_1 = 0.216$ and $H_1 = 1.31$. Then the heat transfer correlation is expressed by

$$Nu_1\dagger\, Ra_I = 0.216\,[Ra_E\,\theta_b]^{1.31}. \tag{32}$$

This equation is in good agreement with equation (28).

From the above-mentioned fact $G_0 \approx G_1$ and $H_0 \approx H_1$. Assumption of $G_0 = G_1 = 0.2$ and $H_0 = H_1 = 1.31$ then yields the following heat transfer expressions:

$$Nu_0\dagger\, Ra_I = 0.2\,[Ra_E(1-\theta_b)]^{1.31}$$

and

$$Nu_1\dagger\, Ra_I = 0.2\,[Ra_E\theta_b]^{1.31}.$$

With a new parameter ϕ, therefore, the heat transfer correlations can be approximated as

$$Nu_0\dagger\left(=\frac{q_0}{QL/2}\right)=\frac{2(1-\theta_b)^{1.31}}{\phi} \tag{33}$$

and

$$Nu_1\dagger\left(=\frac{q_1}{QL/2}\right)=\frac{2\theta_b{}^{1.31}}{\phi} \tag{34}$$

where ϕ is defined as

$$\phi \equiv \frac{Ra_I}{0.1Ra_E^{1.31}}. \tag{35}$$

In other words, $\phi = 0$ and $\phi = 1$ correspond to the external and the internal heating cases, respectively. The combined heating case is located in the domain of $0 < \phi < 1$. From equations (15), (33) and (34), the correlation between θ_b and ϕ is represented by a simple form

$$\phi = \theta_b^{1.31} - (1-\theta_b)^{1.31} \tag{36}$$

Figure 12 shows a comparison of equation (36) with the present experimental data. Although equation (36) predicts slightly smaller values of θ_b than the experimental data, it is very useful for many practical applications since the bulk core temperature can be easily obtained with some degree of accuracy from equation (36) which has only the variable ϕ instead of two independent variables Ra_E and Ra_I.

CONCLUSIONS

An experimental study has been conducted to investigate the effect of bottom heating on thermal turbulent convective heat transfer in a horizontal water layer with volumetric energy sources. Joule heating by alternating current passing through the layer provided the volumetric energy sources. For bottom heating a Nichrome resistance heater was used, which was electrically insulated from the layer. Measurements were made of the temperature distribution in the layer as well as the lower and the upper surface temperatures. Comparison of the experimental results with the boundary layer analysis yielded the following conclusions:

(1) Heat transfer correlations at the lower and the upper surfaces are expressed by equations (27) and (28), respectively.

(2) The bulk core temperature can be easily predicted from equation (36) which has only the variable ϕ derived primarily from the relationship between Ra_I and Ra_E for the internally heated layer with the adiabatic lower surface.

Acknowledgements—The authors wish to express their thanks to Prof. I. Michiyoshi, Kyoto University, for his valuable suggestions and discussions throughout the performance of the present study. Thanks are also expressed to Mr. T. Hori who contributed to the accomplishment of the experiments.

REFERENCES

1. L. Knopoff, *The Earth's Mantle* (edited by T. F. Gaskell), Ch. 8. Academic Press, New York (1967).
2. S. K. Runcorn, Convection currents in the earth's mantle, *Nature, Lond.* **195,** 1248–1257 (1962).
3. D. C. Tozer, Heat transfer and convection currents, *Proc. R. Soc.* **A258,** 252–260 (1966).
4. H. A. Bethe, Energy production in star, *Science, N.Y.* **161,** 541–552 (1968).
5. F. A. Kulacki and M. Z. Nagle, Natural convection in a horizontal fluid layer with volumetric energy sources, *J. Heat Transfer* **97,** 204–211 (1975).
6. H. E. Fiedler and R. Wille, Turbulente Freie Konvektion in Einen Horizontale Flüssigkeitsschicht mit Volumen-Wärmequelle, Paper NC4.5, *Proc. 4th Int. Heat Transfer Conf., Paris* (1970).
7. A. J. Suo-Anttila and I. Catton, The effect of a stabilizing temperature gradient on heat transfer from a molten fuel layer with volumetric heating, *J. Heat Transfer* **97,** 544–548 (1975).
8. F. B. Cheung, Correlation equations for turbulent thermal convection in a horizontal fluid layer heated internally and from below, *J. Heat Transfer* **100,** 416–422 (1978).
9. T. Y. Chu and R. J. Goldstein, Turbulent convection in a horizontal layer of water, *J. Fluid Mech.* **60,** 141–159 (1973).
10. A. M. Garon and R. J. Goldstein, Velocity and heat transfer measurements in thermal convection, *Physics Fluid* **16,** 1818–1825 (1973).
11. A. J. Suo-Anttila and I. Catton, An experimental study of a horizontal layer of fluid with volumetric heating and unequal surface temperature, Paper No. AIChE-5, 16th National Heat Transfer Conf., St. Louis (1976).

CONVECTION THERMIQUE DANS UNE COUCHE DE FLUIDE HORIZONTALE ET CHAUFFEE DANS LA MASSE ET PAR LE BAS

Résumé—On donne les résultats expérimentaux d'une étude de la convection thermique turbulente dans une couche d'eau horizontale avec des sources d'énergie uniformes et volumétriques et avec un chauffage à la base, à flux constant. Les données expérimentales sont comparées avec une analyse simple à couche limite qui exprime les nombres de Rayleigh indépendants, basés respectivement sur le taux de chauffage volumétrique et sur la différence de température entre les surfaces. Une équation pratique est obtenue pour la température moyenne du coeur en fonction d'un paramètre adimensionnel attaché aux niveaux relatifs des chauffages interne et externe.

FREIE KONVEKTION IN EINER VON INNEN UND VON UNTEN BEHEIZTEN HORIZONTALEN FLÜSSIGKEITSSCHICHT

Zusammenfassung—Diese Arbeit behandelt experimentelle Ergebnisse bei turbulenter freier Konvektion in einer horizontalen Wasserschicht mit gleichförmig verteilten volumetrischen Wärmequellen und konstanter Wärmezufuhr von unten. Die Meßdaten wurden mit den Ergebnissen einer einfachen Grenzschichtuntersuchung verglichen, wobei die auf die obere und untere Grenzfläche bezongenen Nusselt-Zahlen als Funktion von zwei unabhängigen Rayleigh-Zahlen ausgedrückt wurden, die sinngemäß mit der volumetrischen Wärmezufuhr und der Temperaturdifferenz zwischen den Oberflächen gebildet wurden. Für die mittlere Flüssigkeitstemperatur wurde eine praktische Korrelationsbeziehung abgeleitet, die von einem einzigen dimensionslosen Parameter abhängt, der die relativen Anteile von innerer und äußerer Wärmezufuhr berücksichtigt.

ТЕПЛОВАЯ КОНВЕКЦИЯ В ГОРИЗОНТАЛЬНОМ НАГРЕВАЕМОМ ИЗНУТРИ И СНИЗУ СЛОЕ ЖИДКОСТИ

Аннотация — Представлены экспериментальные результаты по турбулентной тепловой конвекции в горизонтальном слое воды, содержащем однородно распределенные по объему тепловые источники и нагреваемом снизу с постоянной интенсивностью. Проведено сравнение экспериментальных данных с результатами простого аналитического исследования в приближении пограничного слоя, в котором модифицированные числа Нуссельта для верхней и нижней поверхностей выражались как функции двух независимых чисел Релея, отнесенных соответственно к интенсивности объемного нагрева и разности температур между поверхностями. Выведено практическое критериальное уравнение для определения температуры в центре слоя, зависящей от единственного безразмерного параметра, который характеризует относительную интенсивность внутреннего и внешнего нагревов.